



Journal Homepage: - [www.journalijar.com](http://www.journalijar.com)  
**INTERNATIONAL JOURNAL OF  
 ADVANCED RESEARCH (IJAR)**

Article DOI: 10.21474/IJAR01/4353  
 DOI URL: <http://dx.doi.org/10.21474/IJAR01/4353>



### RESEARCH ARTICLE

#### DIFFUSION-WEIGHTED IMAGING: A FLOURISHING TOOL IN THE DIAGNOSIS OF MAXILLOFACIAL LESIONS.

\*Salma Belal Eiid<sup>1</sup>, Mohamed KhalifaZayet<sup>2</sup> and Mushira Mohamed Dahaba<sup>3</sup>.

1. Assistant lecturer of Oral and Maxillofacial Radiology, Faculty of Oral and Dental Medicine, Cairo University; Cairo, Egypt.
2. Ass. Professor of Oral and Maxillofacial Radiology, Faculty of Oral and Dental Medicine, Cairo University; Cairo, Egypt.
3. Professor of Oral Radiology, Faculty of Oral and Dental Medicine, Cairo University; Cairo, Egypt.

#### Manuscript Info

##### Manuscript History

Received: 26 March 2017  
 Final Accepted: 24 April 2017  
 Published: May 2017

##### Key words:-

Magnetic resonance imaging, Diffusion weighted imaging, ADC map, b-values, MR functional techniques and Maxillofacial lesions.

#### Abstract

**Objective:** The purpose of this study was to address the capability of diffusion-weighted magnetic resonance imaging in the differentiation between maxillofacial lesions.

**Subjects and Methods:** Twenty-five patients with thirty-four lesions were assessed using diffusion-weighted magnetic resonance imaging, and three apparent diffusion coefficient maps were constructed for analysis. The sample was categorized according to the lesion type into benign tumors, cysts, malignancy, inflammatory lesions, fibro-osseous lesions, and giant cell lesions.

**Results:** Statistical analysis revealed that apparent diffusion coefficient map of 300,500,1000 b-values was the most sensitive, and accordingly, a central limit of  $1.42 \times 10^{-3}$  was deduced, separating benign tumor, cyst or infection, from malignancies, giant cell and fibro-osseous lesions.

**Conclusion:** Diffusion weighted imaging seemed to have a great role in differentiation between lesions, and the implementation of different apparent diffusion coefficient maps was of great importance in identification of lesion type

Copy Right, IJAR, 2017., All rights reserved.

#### Introduction:-

The maxillofacial area is a platform for several pathological lesions, and for a lesion to acquire the jaw a real challenge is going to be encountered (Slootweg, 2009). Lesions can have an unseen aggressive tendency, that need a special imaging protocol to foresee this hidden behavior (Razek, 2011; Peacock et al., 2012). In the diagnostic arena, imaging evaluation ranges from the most primitive techniques, i.e., conventional radiography to the more advanced sophisticated type of cross-sectional techniques.

Magnetic resonance imaging (MRI) is one of these techniques, which offers an inherent superior soft tissue contrast resolution, without any hazardous radiation. Nevertheless, MRI is still questioned in terms of its capability of foreseeing the behavior of lesions and defining their nature (Boeddinghaus and Whyte, 2008). Unfortunately, even with combined imaging protocol, diagnosis is still considered unrealistic which, builds a heap of suspicions in the

**Corresponding Author:- Salma Belal Eiid.**

Address:- Assistant lecturer of Oral and Maxillofacial Radiology, Faculty of Oral and Dental Medicine, Cairo University; Cairo, Egypt.

surgeon's mind regarding the lesion nature and till now, biopsy remains the gold standard for diagnosis, which may have its own drawbacks as well (Mohajerani et al., 2009).

Recently, some innovative functional MRI techniques, such as Diffusion Weighted Imaging (DWI), have been capable of providing qualitative image contrast as well as quantitative data by non-invasive depiction of water diffusion within tissues. Diffusion weighted imaging measures the differences in the random displacement of water molecules by the use of the apparent diffusion coefficient (ADC) value (Bozgeyik et al., 2013). In a free medium, there are no boundaries, molecules tend to move and intermingle freely. Conversely, in biological tissues, restricted type of diffusion tends to occur because of the massive amount of cells and barriers found (Punwani, 2010). The sensitivity of diffusion-weighted imaging is controlled by the so-called weighting factor  $b$  or  $b$ -value (Koo et al., 2013). Multiple  $b$ -values can be acquired in a single sequence producing multiple images with different degrees of diffusion sensitivity, which ultimately, allow the formation of the quantitative ADC map (Eida et al., 2007).

The major objective of this study is to examine whether diffusion weighted imaging can be relied on as a tool in providing a crystal-clear suggestion about the disease without the urge for any surgical intervention.

## **Subjects and Methods:-**

### **Patient Population:-**

This research study was carried at the Faculty of Oral and Dental Medicine, Cairo University, where twenty-five patients were collected from its Oral Radiology Outpatient Clinic. The population comprised sixteen males and nine females between 11 and 58 years of age, with an average age 27.4 years with 34 maxillofacial lesions. Before initiating the examination, a written informed consent was signed from each patient or one of his or her guardians. It mentioned clearly that, any extracted information would be registered in a research work, with the patient privacy preserved.

In this work, the exclusion criteria included patients with radiopaque masses, patients who have undergone any sort of surgical interventions prior to scanning, unless a time lag of at least, two weeks was witnessed between the intervention and the scanning time. Moreover, patients who were contraindicated for MRI scanning and lastly, patients who didn't agree to sign the consent.

### **Magnetic resonance examination:-**

Magnetic resonance examination was performed on a 1.5T scanner (Philips, Gyroscan, Intera, Netherlands) using a head coil. An assembled imaging protocol was performed which included, morphological and functional sequences. The morphological sequence used was axial T1-weighted images (TR; 400ms, TE; 15ms), axial T2-TSE (TR; 2500ms, TE; 80ms), with a slice thickness of 4mm using a FOV 180 mm and sagittal or coronal T2-TSE (TR; 2500ms, TE; 100ms) with a slice thickness 3mm and a FOV 155 mm.

DWI was obtained by using the Single-Shot Spin-Echo, Echo-Planar imaging (EPI) technique with four  $b$ -values ( $b = 0, 300, 500, \text{ and } 1000 \text{ s/mm}^2$ ). The imaging parameters were, TR: 3018 ms, TE: 70 ms, and FOV: 180 mm. To improve the signal-to-noise ratio (SNR), eight averages were taken, as well as, applying the sensitivity encoding (SENSE) technique (SENSE factor, 2).

### **Data post-processing:-**

#### **Diffusion weighted image analysis:-**

#### **Diffusion weighted images and ADC maps:-**

By integrating four  $b$  values ( $0, 300, 500 \text{ and } 1000 \text{ s/mm}^2$ ) in the imaging process, three diffusion-weighted images were constructed accordingly. An ADC map<sub>1</sub> ( $0, 300, 500 \text{ and } 1000 \text{ s/mm}^2$ ) was automatically generated on the workstation using the four images. Next, another two ADC maps were manipulated; ADC map<sub>2</sub> of 300, 500, and 1000  $b$ -values and ADC map<sub>3</sub> of 500 and 1000  $b$ -values.

### **Assessment of images and maps:-**

Assessment is a twofold step, where qualitative and quantitative assessments were undertaken. In regards to the qualitative assessment, regions of interest were visually assessed for determining the restriction of tissues.

Restriction was considered only when high signal intensity was registered on  $b$  value  $1000 \text{ s/mm}^2$  and simultaneous

low signal intensity on the gray-scale ADC map, where, R: Restricted (increase in DW signal with simultaneous decrease in ADC map signal), N: Non-restricted (increase in DW signal with simultaneous increase in ADC map signal), and P: Partially restricted (not the whole lesion is restricted). The signal retrieved is correlated to the restricted signal of the parotid glands or the spinal cord according to the level of the slice. Regarding the quantitative assessment, the ADC values of the three ADC maps were recorded.

#### Colored ADC map:-

The conventional DICOM gray-scale ADC map was converted to colored ADC map using OSIRIX software, which was downloaded on a Macintosh personal computer from (<http://www.osirix-viewer.com>). Owing to this OSIRIX, color maps are easily manipulated, where a "CLUT (Color Look up Table)" tool was used and the "Spectrum" option was chosen. Thereafter, the window level of the color-scale ADC map images was set at  $1.5 \times 10^2$  mm<sup>2</sup>/s and the window width at  $3.0 \times 10^2$  mm<sup>2</sup>/s. Areas having high ADCs are displayed as red and as ADC value decreases, the color degrades to yellow or green or blue, blue color is the one with the lowest ADC value (Fig 1). The lesions were described as lesions: with reddish tint(1), with yellowish tint (2), or green(3), or blue(4) lesions.

#### Histo-pathological Investigation:-

Histo-pathological diagnosis was established for all investigated cases.

#### Statistical analysis:-

Statistical analysis was performed with SPSS 20.0 (Statistical Package for Scientific Studies) for windows (SPSS, Inc., an IBM Company USA). The sample in this work was categorized according to the type of the lesion. First of all, Kruskal-Wallis One Way Analysis of Variance on ranks was used for measuring the significance of the MRI parameters for different lesion types. Subsequently, Multiple regression analysis was applied to weigh parametersthat were significant. Analysis of means (ANOM) plot was needed to acquire a threshold value for differentiation between lesion types. Moreover, Pair-wise comparison of significant ANOVA (Holm-Sidak method) for differentiation between ADC map<sub>1</sub> and ADC map<sub>3</sub> was applied.

#### Results:-

According to the first classification mode applied in the current work, the investigated sample comprised thirteen benign odontogenic tumors, five inflammatory lesions, six cysts, three malignancies, three fibro- osseous lesions, and four giant cell lesions. Meanwhile, in the second classification mode the sample was simply categorized into nine aggressive lesions (all malignancies, three ameloblastomas, one myxoma, one calcifying epithelial odontogenic tumor, and one keratocystic odontogenic tumor), whereas, non-aggressive embraced the rest of the sample.

The results of Kruskal-Wallis One Way Analysis of Variance on ranks revealed that four out of the five assessed parameters (Table 1) changed significantly between the different lesions types. And according to the results of ANOVA in the multiple regression analysis, the highest contributing factor was ADC map<sub>2</sub>. No statistical significant difference was encountered for any lesion type between different ADC maps. However, the differences in the mean values among the three ADC maps for the malignant group was greater than would be expected. The results of pair-wise comparison of significant ANOVA (Holm-Sidak method) revealed a significant difference between ADC map<sub>1</sub> and ADC map<sub>3</sub>.

Analysis of means (ANOM) plot with 95% confidence interval was used and showed that ADC 1 values, ADC 2 values, and ADC 3 values ( $\times 10^{-3}$ ) were able to discriminate benign, cysts, and infection as a category from malignancy, fibro-osseous and giant cell lesions with central limit values of 1.53, 1.42, and 1.36 respectively (Fig 2).

#### Discussion:-

There is a wealth of imaging approaches available for maxillofacial imaging, each can deliver a specific type of data, however each of which has its own inherent defect. Therefore, potential synergy between different techniques is now more desirable to increase the scope of tissue examination (Sasaki and Nakamura, 2010).

In this study, an imaging protocol was customized by incorporating one of the state-of-art functional techniques (Diffusion-weighted MR imaging) with conventional morphological techniques as T1WI and T2WI. The

results regarding the first mode showed that four from the five parameters; the ADC values of the three maps, and a colored ADC map changed significantly between the lesions according to ANOVA, whereas, restriction had no value in such discrimination. This was not in concordance with the theory proposed by Whittaker et al 2009 and such discrepancy in results may be due to the small sized sample in our work.

In this work, the purpose from formulating different maneuvered maps was to obtain an ADC map with the highest significance, as well as an attempt to assess the perfusion in lesions using DWI. According to this study, ADC map<sub>2</sub> showed the highest significance. Comparison between ADC 1, 2, and 3 threshold values were made using the ANOVA. Surprisingly, no statistical significant difference was encountered between the different ADC maps. Nonetheless, the results of Holm-Sidak method revealed a significant difference between ADC 1 and ADC 3 in malignant lesions. This significant discrepancy in malignancy values should be attributed to the angiogenesis phenomenon, which is dominant in aggressive malignant lesions.

The ADC map<sub>3</sub> is the end result of b-value 500 and 1000 excluding the 0 and 300 b-values, which automatically exclude perfusion as well with final decrease in ADC calculation. Therefore, in this study, above b-value 300, is advocated to exclude the perfusion of tissues, which was previously declared by Nilsen et al 2013.

This study corroborated several results reported in the literature as Ceçe et al 2013, Eida et al 2007, and Sumi et al 2008, where lesions of high cellularity, as malignant lesions, showed the lowest ADCs, whereas, lesions of freely diffusing molecules, showed the highest values. In this work, cyst values were not consistent with others (Abdel Razek et al., 2009; Sakamoto et al., 2009; Sumi et al., 2008; Wang et al., 2001). Cyst showed lower results, since the investigated sample did not solely comprise simple cysts but it included two dentigerous and two glandular odontogenic cysts while others were primarily performed on simple cysts. It was reported that dentigerous cysts seem to be more heterogeneous than cystic areas in ameloblastoma and simple cysts (Sumi et al., 2008). And regarding, the glandular odontogenic cyst content, it was claimed that these cysts may contain mucous that will decrease diffusivity within the lesion (Kaplan et al., 2008).

Moreover, infection findings were inconsistent with other findings, where infection in general seems to give low ADC values because of the influx of inflammatory cells as well as the pus congestion in the area to be assessed (Koç et al., 2007). Our infection sample comprised only infected cysts, which ultimately affected the reliability of the results.

Colored ADC map seemed to be sensitive in tissue heterogeneity assessment as well as differentiation between the lesions, where most benign lesions showed a green color, cysts were either green-yellow or red, malignancy were only blue (100%), 75% of giant cell lesions were blue, fibro-osseous were only green in color, whereas, infection gave a range of color spectrum depending on the level of inflammation.

Thus far, there have been few studies which performed colored ADC maps on lesions, and although they were not analogous to our work, however, these two studies, Eida et al 2007 and Sumi et al 2008 acknowledged that colored ADC maps can depict different histopathological tissues and proved efficiency in differentiation between ameloblastoma and keratocystic odontogenic tumor, which in a way supported our results.

According to ANOM plot, a central limit of  $1.42 \times 10^{-3}$  was deduced, where above it is most probably a cyst, benign, or infection and below it seemed to be a fibro-osseous, giant cell lesions, or malignancy. There seems to be a gap, however, in literature regarding this wide classification, where most of the authors as Srinivasan et al 2008, Razek et al 2008 and Nakahira et al 2012 studied the differentiation between benign and malignant. And the others focused primarily on certain lesions or certain categories as the differentiation between ameloblastoma and keratocystic odontogenic tumour (Sumi et al., 2008), and lymphomas versus carcinomas (Ichikawa et al., 2012).

Over the past decade, new MR techniques and interpretation strategies have been developed to increase our perception for diagnosis. MRI can be made more vivid when incorporating the so-called functional techniques in the imaging protocol. According to this study conditions and limitations, it was inferred that there are certain parameters that may have an impact in such differentiation as ADC map<sub>2</sub> (300, 500, and 1000), which was the most sensitive

contributor in difference recognition. Diffusion weighted imaging appeared to be a great establishment to rely on in the coming future, and its addition to the conventional MRI is such a treasure. Although the implementation of ADC map<sub>2</sub> is crucial, nevertheless, it was concluded that the integration of ADC map<sub>1</sub> with b-values (0,300, 500, and 1000) and ADC map<sub>3</sub> (500 and 1000) is advocated, since it gave an indication about the lesion perfusivity, which is directly correlated to aggressiveness. Moreover, one of the imperative parameters was the colored ADC map, which was of great help and served as a reliable tool in differentiation between different categories.

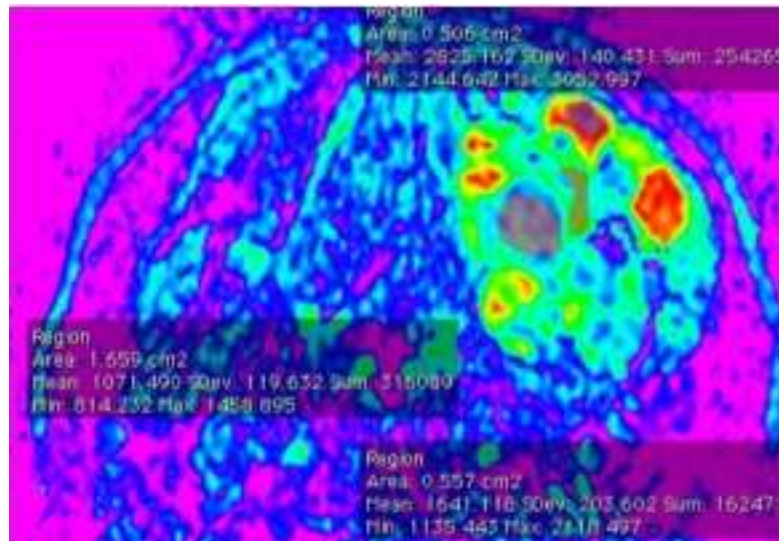


**Figure 1:-** A colored ADC map showing vividly the different tissues within an ameloblastoma, where cystic areas gave a red color with an ADC value of 2.82, cellular dense areas gave a blue color of 1.07 ADC value, and the separating fibrous tissues showed a green color of 1.64 ADC value.

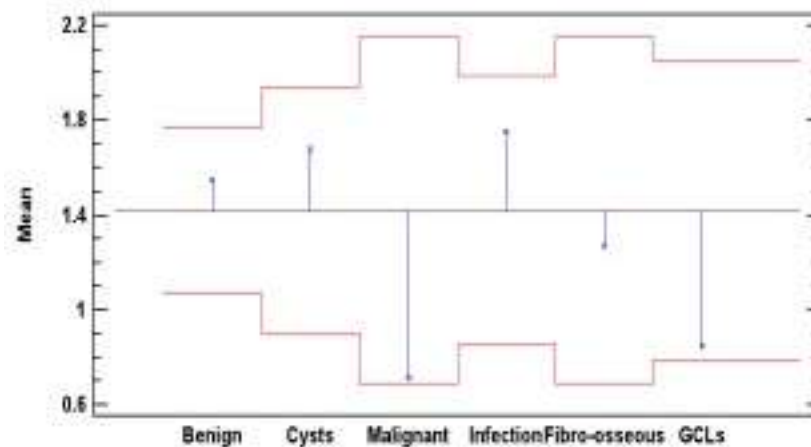


**Figure 2:-** Analysis of means (ANOM) plot with 95% confidence interval ADC 2 values ( $\times 10^{-3}$ ) for the different lesion types.

**Table 1:-** Analysis of variance of the DW parameters assessed for the different lesions types:

DW parameters	P-value	Sig
Restriction	0.315	NS
ADC value 1 ( $\times 10^{-3}$ )*	0.001	S
ADC value 2 ( $\times 10^{-3}$ )*	0.018	S
ADC value 3 ( $\times 10^{-3}$ )*	0.037	S
Color map	0.027	S

\*: Values are Numerical in nature, NS: non-significant, S: significant

**Acknowledgment:** No source of funding.

## References:-

1. Abdel Razek, A. A. K., Gaballa, G., Elhawarey, G., Megahed, A. S., Hafez, M., & Nada, N. (2009). Characterization of pediatric head and neck masses with diffusion-weighted MR imaging. *EurRadiol*, 19(1), 201–8. doi:10.1007/s00330-008-1123-6
2. Bitar, R., Leung, G., Perng, R., Tadros, S., Moody, A. R., Sarrazin, J., ... Roberts, T. P. (2006). MR pulse sequences: what every radiologist wants to know but is afraid to ask. *Radiographics : A Review Publication of the Radiological Society of North America, Inc*, 26(2), 513–37. doi:10.1148/rg.262055063
3. Boeddinghaus, R., & Whyte, A. (2008). Current concepts in maxillofacial imaging. *Eur J Radiol*, 66(3), 396–418. doi:10.1016/j.ejrad.2007.11.019
4. Bozgeyik, Z., Onur, M. R., & Poyraz, A. K. (2013). The role of diffusion weighted magnetic resonance imaging in oncologic settings. *Quant Imaging Med Surg*, 3(5), 269–78. doi:10.3978/j.issn.2223-4292.2013.10.07
5. Ceçe, H., Gündoğan, M., Karakaş, O., Karakaş, E., Boyacı, F. N., Yıldız, S., ... Seker, A. (2013). The role of diffusion-weighted magnetic resonance imaging in the classification of hepatic hydatid cysts. *Eur J Radiol*, 82(1), 90–4. doi:10.1016/j.ejrad.2012.08.015
6. Eida, S., Sumi, M., Sakihama, N., Takahashi, H., & Nakamura, T. (2007). Apparent diffusion coefficient mapping of salivary gland tumors: prediction of the benignancy and malignancy. *AJNR. Am J Neuroradiol*, 28(1), 116–21. Retrieved from <http://www.ncbi.nlm.nih.gov/pubmed/17213436>
7. Ichikawa, Y., Sumi, M., Sasaki, M., & Sumi, T. (2012). Efficacy of Diffusion-Weighted Imaging for the Differentiation between Lymphomas and Carcinomas of the Nasopharynx and Oropharynx : Correlations of Apparent Diffusion Coefficients and Histologic Features. *AJNR Am J Neuroradiol*, 33(4), 761–766.
8. Kaneda, T. (2003). MR imaging of maxillomandibular lesions. *Oral Radiol.*, 19(1), 64–69.
9. Kaplan, I., Anavi, Y., & Hirshberg, a. (2008). Glandular odontogenic cyst: a challenge in diagnosis and treatment. *Oral Dis*, 14(7), 575–81. doi:10.1111/j.1601-0825.2007.01428.x
10. Koç, O., Paksoy, Y., Erayman, I., Kivrak, A. S., & Arbag, H. (2007). Role of diffusion weighted MR in the discrimination diagnosis of the cystic and/or necrotic head and neck lesions. *Eur J Radiol*, 62(2), 205–13. doi:10.1016/j.ejrad.2006.11.030
11. Koo, J. H., Kim, C. K., Choi, D., Park, B. K., Kwon, G. Y., & Kim, B. (2013). Diffusion-Weighted Magnetic Resonance Imaging for the Evaluation of Prostate Cancer: Optimal B Value at 3T. *Korean J Radiol : Official Journal of the Korean Radiological Society*, 14(1), 61–69. doi:10.3348/kjr.2013.14.1.61
12. Mohajerani, H., Mosalman, M., Mohajerani, S. A., & Ghorbani, Z. (2009). Frequency of Giant Cell Lesions in Oral Biopsies. *J Dent (Tehran)*, 6(4), 193–197.
13. Nakahira, M., Saito, N., Murata, S., Sugawara, M., Shimamura, Y., Morita, K., ... Matsumura, S. (2012). Quantitative diffusion-weighted magnetic resonance imaging as a powerful adjunct to fine needle aspiration cytology for assessment of thyroid nodules. *Am J Otolaryngol*, 33(4), 408–16. doi:10.1016/j.amjoto.2011.10.013
14. Nilsen, L. B., Fangberget, A., Geier, O., & Seierstad, T. (2013). Quantitative analysis of diffusion-weighted magnetic resonance imaging in malignant breast lesions using different b value combinations. *EurRadiol*, 23(4), 1027–33. doi:10.1007/s00330-012-2687-8
15. Peacock, Z. S., Resnick, C. M., Susarla, S. M., Faquin, W. C., Rosenberg, A. E., Nielsen, G. P., ... Kaban, L. B. (2012). Do Histologic Criteria Predict Biologic Behavior of Giant Cell Lesions? *J Oral Maxillofac Surg : Official Journal of the American Association of Oral and Maxillofacial Surgeons*, 1–8. doi:10.1016/j.joms.2011.12.005
16. Punwani, S. (2010). Diffusion weighted imaging of female pelvic cancers: concepts and clinical applications. *Eur J Radiol*, 78(1), 21–9. doi:10.1016/j.ejrad.2010.07.028
17. Razek, a a K. A., Sadek, a G., Kombar, O. R., Elmahdy, T. E., & Nada, N. (2008). Role of apparent diffusion coefficient values in differentiation between malignant and benign solitary thyroid nodules. *AJNR. Am J Neuroradiol*, 29(3), 563–8. doi:10.3174/ajnr.A0849
18. Razek, A. A. K. A. (2011). Imaging appearance of bone tumors of the maxillofacial region. *World J Radiol*, 3(5), 125–34. doi:10.4329/wjr.v3.i5.125
19. Sadick, M., Schoenberg, S. O., Hoermann, K., & Sadick, H. (2012). Current oncologic concepts and emerging techniques for imaging of head and neck squamous cell cancer. *GMS Current Topics in Otorhinolaryngology, Head and Neck Surgery*, 11, Doc08. doi:10.3205/cto000090

20. Sakamoto, J., Yoshino, N., Okochi, K., Imaizumi, A., Tetsumura, A., Kurohara, K., & Kurabayashi, T. (2009). Tissue characterization of head and neck lesions using diffusion-weighted MR imaging with SPLICE. *Eur J Radiol*, 69(2), 260–8. doi:10.1016/j.ejrad.2007.10.008
21. Sasaki, M., & Nakamura, T. (2010). Pixel-based time–intensity curve analysis and apparent diffusion coefficient mapping of sinonasal organized hematomas. *Oral Radiol*, 26(2), 101–105. doi:10.1007/s11282-010-0042-9
22. Slootweg, P. J. (2009). Lesions of the jaws. *Histopathology*, 54(4), 401–18. doi:10.1111/j.1365-2559.2008.03097.x
23. Srinivasan, a, Dvorak, R., Perni, K., Rohrer, S., SK, M., & Mukherji, S. K. (2008). Differentiation of benign and malignant pathology in the head and neck using 3T apparent diffusion coefficient values: early experience. *AJNR. Am J Neuroradiol*, 29(1), 40–4. doi:10.3174/ajnr.A0743
24. Sumi, M., Ichikawa, Y., Katayama, I., Tashiro, S., & Nakamura, T. (2008). Diffusion-weighted MR imaging of ameloblastomas and keratocystic odontogenic tumors: differentiation by apparent diffusion coefficients of cystic lesions. *AJNR Am J Neuroradiol*, 29(10), 1897–901. doi:10.3174/ajnr.A1266
25. Wang, J., Takashima, S., Takayama, F., Kawakami, S., Saito, A., Matsushita, T., ... Ishiyama, T. (2001). Head and neck lesions: characterization with diffusion-weighted echo-planar MR imaging. *Radiology*, 220(3), 621–630. Retrieved from <http://search.bvsalud.org/portal/resource/en/mdl-11526259>
26. Whittaker, C. S., Coady, A., Culver, L., Rustin, G., Padwick, M., & Padhani, A. R. (2009). Diffusion-weighted MR imaging of female pelvic tumors: a pictorial review. *Radiographics: A Review Publication of the Radiological Society of North America, Inc*, 29(3), 759–74; discussion 774–8. doi:10.1148/rg.293085130